Impedance Compensation of SUBAR for Back-Drivable Force-Mode Actuation

Kyoungchul Kong, *Student Member, IEEE*, Hyosang Moon, *Student Member, IEEE*, Beomsoo Hwang, *Student Member, IEEE*, Doyoung Jeon, *Member, IEEE*, and Masayoshi Tomizuka, *Fellow, IEEE*

***Abstract*—The Sogang University biomedical assistive robot (SUBAR), which is an advanced version of the exoskeleton for patients and the old by Songang (EXPOS) is a wearable robot developed to assist physically impaired people. It provides a person with assistive forces controlled by human intentions. If a standard geared dc motor is applied, however, the control efforts will be used mainly to overcome the resistive forces caused by the friction, the damping, and the inertia in actuators. In this paper, such undesired properties are rejected by applying a flexible transmission. With the proposed method, it is intended that an actuator exhibits zero impedance without friction while generating the desired torques precisely. Since the actuation system of SUBAR has a large model variation due to human–robot interaction, a control algorithm for the flexible transmission is designed based on a robust control method. In this paper, the mechanical design of SUBAR, including the flexible transmission and its associated control algorithm, are presented. They are also verified by experiments.**

***Index Terms*—Exoskeleton, force-mode actuation, human–robot interaction, mechanical impedance.**

I. Introduction

EXOSKELETON for patients and the old by Sogang [EXPOS; see Fig. 1(a)] is a human-centered robot developed to assist people with walking problems [1], [2]. For easy use of the device, the system is constituted by a caster walker and a wearable part that has a minimal weight. The assistive power is transferred by the tendon mechanism; the force is transmitted from the caster walker to each hip and knee joint of wearable part through flexible wires and pulleys. Recently, we have designed an advanced version, which is known as the Sogang University biomedical assistive robot [SUBAR; see Fig. 1(b)], with an improved actuating power and a transmission mechanism for more effective assistance. The detailed specifications are compared in Table I.

Mechanical impedance plays an important role in the design of robots that physically interact with a human. If the mechanical impedance is large, the motions of the overall system (i.e., a human body wearing a robot) are dominated by the robot. Therefore, large mechanical impedance is undesirable in terms of safety and comfort, and it is required to be minimized for the ideal human–robot interaction [7]. In reality, actuators with large actuation power usually show large mechanical impedance due to the friction and the inertia. Therefore, the selection of a proper actuator in terms of the actuation capability and the mechanical impedance is a very challenging problem. Sometimes the impedance is actively controlled for particular purposes (e.g., the control of semiactive actuators for rehabilitation processes [5], [6]), but it does not mean that the mechanical impedance can be large, i.e., the impedance should be purely generated by an actuator force. Note that the small mechanical impedance is of unique requirements for physical human–robot interaction; actuators for industrial applications are required to have large mechanical impedance for a good disturbance rejection performance.

(a) (b)

Fig. 1. Assistive robots developed by Sogang University. (a) EXPOS [1], [2]. (b) SUBAR.

TABLE I
Hardware Specification

	EXPOS	SUBAR
Max. Torque [Nm]	7.7	44.0
Number of Active Joints	4 (Hip and Knee Joints)	4
Weight of Wearable Part [Kg]	3.2	11.0

Manuscript received September 11, 2008; revised February 20, 2009 and March 19, 2009. First published May 8, 2009; current version published June 5, 2009. This paper was recommended for publication by Associate Editor M. Johnson and Editor K. Lynch upon evaluation of the reviewers' comments. This work was supported in part by the National Science Foundation under Grant CMMI-0800501 and in part by the Intelligent Robotics Development Program, which is one of the 21st Century Frontier R&D Programs supported by the Ministry of Knowledge Economy of Korea.

K. Kong and M. Tomizuka are with the Department of Mechanical Engineering, University of California, Berkeley, CA 94720 USA (e-mail: kckong@me.berkeley.edu; tomizuka@me.berkeley.edu).

H. Moon, B. Hwang, and D. Jeon are with the Department of Mechanical Engineering, Sogang University, Seoul, Korea 121-742 (e-mail: hsmoon@sogang.ac.kr; bshwang@sogang.ac.kr; dyjeon@sogang.ac.kr).

Color versions of one or more of the figures in this paper are available online at http://ieeexplore.ieee.org.

Digital Object Identifier 10.1109/TRO.2009.2019786

Since the worn part of EXPOS has minimal weight and is connected to lightly geared motors, it has small mechanical impedance, and the actuators are back-drivable. In the case of SUBAR, however, the mechanical impedance has been increased significantly as the gear reduction ratio has been increased for more powerful assistance. This means that the SUBAR is not directly applicable for physically impaired people who need very precise assistance.

The main controller of SUBAR determines the magnitude and the direction of assistive forces to augment human power. However, if disturbances are imposed on the system, they may also be amplified, and the human may feel discomfort [3], [4]. Therefore, it is necessary to reject the undesired disturbances for precise and comfortable assistance. Since it is hard to distinguish the disturbances from the force intended by a human, an additional controller that rejects the disturbance selectively is introduced to SUBAR in this paper. In this case, the primary disturbances are forces generated by the friction, the damping, and the inertia in actuators, which are also the major sources that increase the mechanical impedance.

In order to reduce the mechanical impedance in applications of physical human–robot interaction, various approaches have been proposed. Buerger and Hogan introduced an impedance compensator based on a loop shaping method to have the desired impedance behavior [7]. Blaya and Herr [8], Pratt *et al*. [14], and Pratt and Williamson [15] applied series elastic actuator (SEA), which consists of a linear spring and an electric motor. It provides a solution to reduce the mechanical impedance, but the control algorithm has not been fully developed. In this aspect, the rotary SEA (RSEA) and its control method developed by Kong and Tomizuka are noteworthy [9]–[11]. Two rotary encoders on each side of a spring measure the deflection of the spring, by which the desired torque output is generated. With a well-designed servo controller, the actuator including the flexible transmission exhibits very low mechanical impedance.

To compensate for the mechanical impedance of SUBAR, the mechanism of the RSEA is applied in this paper. For the design of the controller that rejects the undesired disturbances selectively, the dynamic characteristics of actuators in SUBAR, which are related to the mechanical impedance (e.g., the resistive torques and the input–output linearity) are analyzed quantitatively. Based on the analysis, a controller that robustly controls the flexible transmission is designed and verified by experiments.

This paper is organized as follows. Hardware design of SUBAR and its basic characteristics are discussed in Section II. In Section III, the design of a control algorithm for rejecting the undesired disturbances is introduced. The proposed methods are verified by experiments in Section IV. A conclusion and future work are given in Section V.

II. System Configuration of SUBAR

A. Mechanical Design Concepts

EXPOS was designed by minimizing the weight and volume of the worn part for easy use of the device [1], [2]. A caster walker was introduced to carry all of the heavy peripherals including actuators, batteries, and controllers, as shown in Fig. 1(a). The assistive force is transferred via a tendon mechanism. Since the caster walker and worn part can be disassembled easily, patients may easily put on and take off the device.

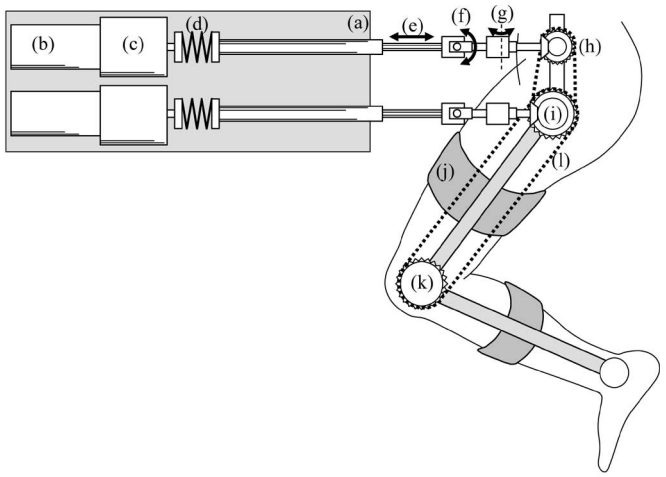

Fig. 2. Schematic plot of the power transfer mechanism. (a) Robot arm of the SUBAR [see Fig. 3(a)]. (b) DC motors for assisting joints. (c) Gear boxes. (d) Flexible transmission. (e) Sliding shaft, which provides 1 DOF for a natural human motion. (f) and (g) Universal joints, which also provide degrees of freedom for natural human motion. (h) Sprocket for hip joint assistance (disconnectable from the robot arm). (i) Sprocket for knee joint assistance (disconnectable from the robot arm). (j) Brace. (k) Sprocket of knee joint. (l) Chain.

For assisting people with severe impairments, it is necessary to provide sufficiently large torques. Since the maximum torque of the EXPOS is not large enough to assist such users, the actuation power has been increased significantly in the design of the SUBAR. In order to transfer the large torque, the tendon mechanism is replaced by the chain and gear mechanism. A schematic plot of the power transfer mechanism is shown in Fig. 2. To guarantee the degrees of freedom required for the natural walking, various mechanical power transmissions such as the sliding shaft [see Fig. 2(e)] and the universal joint [see Fig. 2(f) and (g)] are utilized, as shown in the figure.

In each robot arm of the caster walker, two motors that assist hip and knee joints are installed, as shown in Fig. 2(a).

Due to the high reduction ratio, the mechanical impedance of SUBAR has been increased significantly. In order to improve the preciseness of assistance by reducing the impedance, a flexible transmission is installed, as shown in Fig. 3. The transmission consists of a torsion spring, two rotary encoders at each side of the spring, and a hardware angle limiter shown in Fig. 3(c). The torsion spring plays a role of an energy buffer between the actuator and the human joint, as well as a torque measurement unit. The torque generated by the actuator is transferred to a torsion spring and stored as elastic energy. The assistive torque is generated via the release of the energy stored in the spring. By controlling the spring deflection precisely, SUBAR may generate the desired torque with low impedance.

B. Characteristics of Actuation System

In order to measure the mechanical impedance of the actuator, an experiment was set up, as shown in Fig. 4(a). The actuator in

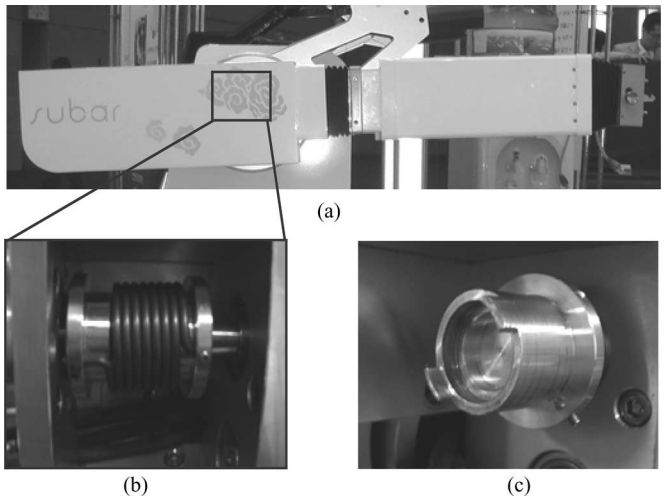

Fig. 3. Flexible transmission installed in the SUBAR. (a) Robot arm of the SUBAR. (b) Flexible transmission. (c) Mechanical angle limiter.

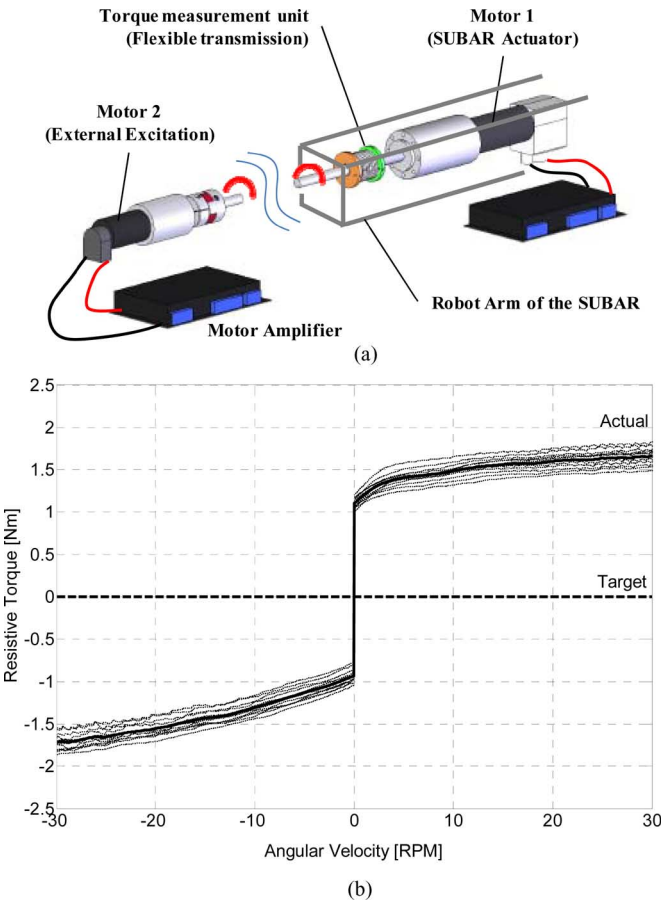

Fig. 4. Actuator impedance test. (a) Experimental setup for testing resistive torque of the actuator. (b) Experimental results. Thick continuous line represents the average values.

SUBAR (motor 1 in the figure) was in the torque mode. An additional motor (motor 2 in the figure) was installed to exert precise external excitations. Fig. 4(b) shows the experimental results. To find the relation between the resistive torque and the angular velocity, the torque command to motor 1 was set to zero. Note that

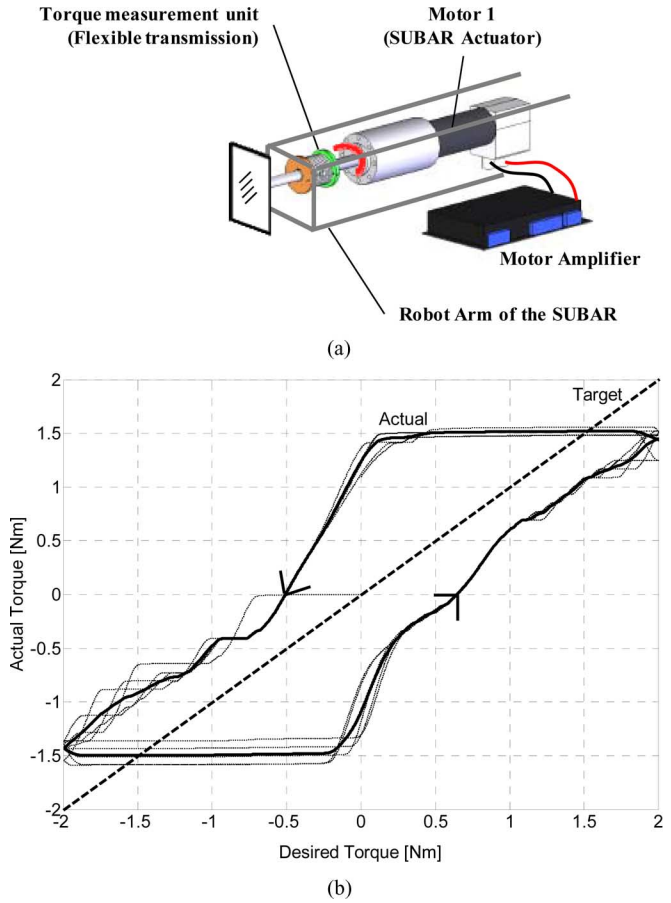

Fig. 5. Linearity test of the actuator. (a) Experimental setup for testing linearity of torque output. (b) Experimental results. Thick continuous line represents the average values.

the actuator has large resistive torque (see actual in the figure), which is caused mainly by the static friction and the damping effect. Suppose that the actuator is directly connected to a human joint without any compensation mechanism or algorithm. The human may be disturbed by the resistive forces shown in Fig. 4 and may not feel the correct assistive force. Therefore, it is necessary to introduce an additional mechanism or algorithm, such as the RSEA proposed in [11], to avoid this problem.

Fig. 5 shows the experimental setup and results for testing the linearity of the torque output. To observe the relation between the generated torque and the desired torque, the load side of the flexible transmission was mechanically locked to make the angular velocity zero. As shown in Fig. 5(b), the torque output does not follow the command correctly and exhibits large hystereses (see actual in the figure). Since this may cause uncomfortable feeling during assistance, the undesired characteristics, as shown in Figs. 4 and 5, should be rejected by applying a compensation algorithm.

III. Design of Servo Controller for Flexible Transmission

For simplicity, it is assumed that the spring installed in the flexible transmission is linear. The spring deflection is to be

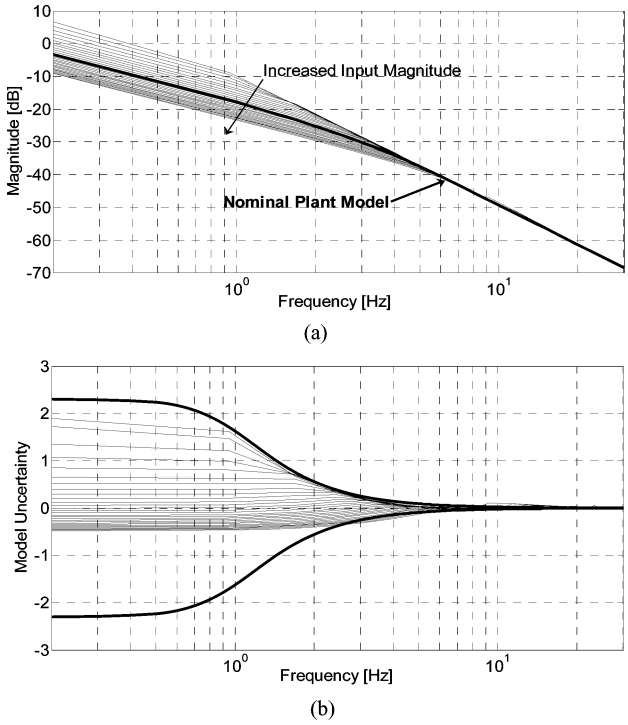

Fig. 6. System identification of the actuation system in the SUBAR. (a) Frequency responses. (b) Multiplicative model uncertainties. The dashed lines represent the magnitude of the boundary function of uncertainties.

controlled such that the desired torque can be generated by the proper offset. For example, when the desired assistive torque is zero, the actuator is controlled to follow the human motion without the spring deflection.

A. Actuator Dynamics Modeling

In order to design a robust tracking controller that satisfies the performance objectives (i.e., the precise control of the spring deflection), the model of actuation system was identified by frequency responses, as shown in Fig. 6. The amplitude of the sinusoidal excitation was varying from 0.1 to 5 V. It should be noted that the system has a large nonlinearity, such as velocity saturation and friction, so that it shows different frequency responses according to the input magnitudes. Also, the system shows large model variations in low frequencies [see Fig. 6(a)] due to the velocity limitation of the actuator.

The thick continuous line in Fig. 6(a) represents the nominal model $G_n(s)$. It was obtained by averaging the magnitudes of the frequency responses. Since the system is subjected to large model variations, a multiplicative model uncertainty is introduced to the nominal model, i.e.,

$$G_a(s) \in \tilde{G}(s) = G_n(s)[1 + W(s)\Delta(s)] \tag{1}$$

where $G_a(s)$ is an actual model of the system, $\tilde{G}(s)$ is a possible model set, $W(s)$ is a stable and proper boundary function of the model uncertainties, and $\Delta(s)$ is any arbitrary stable transfer function with the bounded magnitude, i.e., $\|\Delta\|_\infty < 1$. Since the magnitude and the phase of $G_a(j\omega)$ and $G_n(j\omega)$ are known (i.e., $G_n(s)$ was designed and those of $G_a(j\omega)$ were measured),

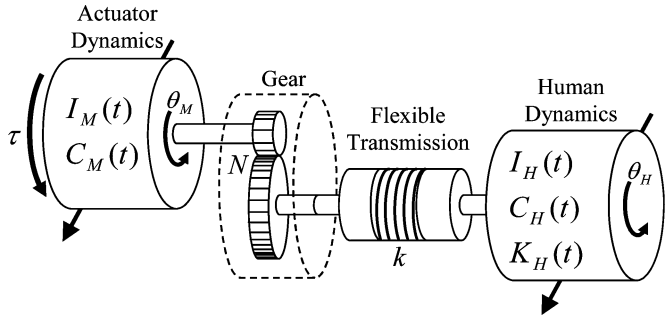

Fig. 7. Schematic plot of a motor interacting with a human.

$W(j\omega\Delta(j\omega)$ is obtained by simple calculations in the complex domain, i.e.,

$$W(j\omega)\Delta(j\omega) = \frac{G_a(j\omega) - G_n(j\omega)}{G_n(j\omega)}. \tag{2}$$

Fig. 6(b) shows the multiplicative uncertainties calculated by (2) for each experiment. As expected, the uncertainties are mainly at low frequencies. Since $|\Delta(j\omega)|$ is bounded to one, the maximum $|W(j\omega)\Delta(j\omega)|$ is equal to $|W(j\omega)|$ for all frequencies ω. Therefore, $W(s)$ is designed such that all of the magnitudes of multiplicative uncertainties are in the region of $\pm|W(j\omega)|$, as shown in Fig. 6(b).

B. Model Variation by Human–Robot Interaction

Since SUBAR interacts with a human, the human body dynamics may affect the overall system dynamics. Therefore, it is necessary to assure that the controller stably and robustly controls the flexible transmission under the environment interacting with a human. However, the human body dynamics are difficult to model due to their complexity and time-varying nature, which depends on the phases of human motion (e.g., the change of ground contact points).

Fig. 7 shows a schematic plot for modeling the actuation system interacting with a human. Actuator dynamics including the gear was analyzed by frequency responses in the previous section. As discussed before, the linearized parameters of the actuator (i.e., $I_M(t)$ and $C_M(t)$ in Fig. 7) are time-varying due to nonlinearities and interaction with a human. The torque generated by the actuator is amplified by a gear and transferred to a human joint via the flexible transmission. It is assumed that the gear is an ideal transformer that has neither energy loss nor inertia. In the figure, k represents a spring constant of the flexible transmission, and $I_H(t)$, $C_H(t)$, and $K_H(t)$ represent an inertia, a damping coefficient, and a coefficient related to the gravity of a human body segment, respectively. A human body is a multilink system that has very complicated and coupled dynamics. The dynamic characteristics are also dependant on the ground contact points. For example, dynamics of a swinging leg are different from those of a leg touching the ground. Therefore, the parameters of the human part in a linear model, which are shown in Fig. 7, are also time-varying.

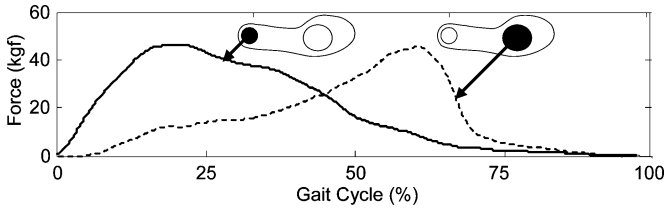

Fig. 8. Ground contact forces for one gait cycle.

Equation of motion for the actuator, including the gear and the flexible transmission, is

$$I_M\ddot{\theta}_M + C_M\dot{\theta}_M = \tau - \frac{k}{N}\left(\frac{\theta_M}{N} - \theta_H\right). \tag{3}$$

For simplicity, (t) of each parameter is ignored in (3). Dynamic equation of the human part is

$$I_H\ddot{\theta}_H + C_H\dot{\theta}_H + K_H\theta_H = k\left(\frac{\theta_M}{N} - \theta_H\right) \tag{4}$$

where the exogenous disturbance in the human part, i.e., the human muscular force, is neglected in (4). Combining (3) and (4), the transfer function from the motor torque to the motor position is obtained as

$$\frac{\theta_M(s)}{\tau(s)} = \frac{1}{I_M s^2 + C_M s + kN^{-2}\alpha(s)} \tag{5}$$

where

$$\alpha(s) = \frac{I_H s^2 + C_H s + K_H}{I_H s^2 + C_H s + K_H + k}. \tag{6}$$

Note that the parameters related to the human part are included only in $\alpha(s)$, and the effect of the human body dynamics is attenuated by N^{-2} in (5). This is an advantage gained by increasing the gear ratio. If $N \to \infty$, the actuator system is not affected by the human body dynamics. Note that the human body dynamics part in (5) [i.e., $\alpha(s)$] has the bounded magnitude over the entire frequency range. Since N is large enough ($N = 71$) and the spring constant k of the flexible transmission is not that large ($k = 0.9$ Nm/°) in the case of SUBAR, it is assumed that the human body dynamics do not affect the actuator dynamics for the sake of simplicity.

Even though the human body dynamics can be neglected when the change of dynamic characteristics is slow, instability can be introduced if the change of the dynamic characteristics is drastic (e.g., an impulsive release of stored energy). Dynamic characteristics of a human body depend on phases in human motions. In normal conditions, the motion phases change smoothly and continuously to protect the body from impact forces. The theoretical proof related to the change of motion phases is not given in this paper, because human nature is not modeled easily. However, it is possible to experimentally verify the smooth and continuous change of the motion phases by measuring the ground contact forces from the soles of the shoes [13]. Since human body dynamics are mainly dependant on the location of ground contact points, the motion phases may be smoothly changed if the change of ground contact forces is smooth and continuous. As shown in Fig. 8, the ground contact forces change smoothly and continuously, which implies that the change of the human body dynamics is smooth and continuous as well. For more detailed information about human motion phases, see [13].

C. Design of Servo Controller for Flexible Transmission

Considering the large model variation of the system, the controller of the flexible transmission applies the disturbance observer (DOB). The concept of the control algorithm and the approach in [11] are adopted in this paper. In general, the DOB may be used to

1) estimate and cancel disturbance;
2) compensate for the variation of plant dynamics by treating the variation as an equivalent disturbance.

In this application, the DOB is used more for the second objective although the disturbance cancellation is also taking place.

In the design of the DOB, it is important to select the Q-filter. The first requirement is that the order of Q(s) must be selected so that $Q(s)G_n^{-1}(s)$ is realizable. The remaining two conditions make the closed-loop system with DOB robust in terms of performance and stability. Namely, the DOB is effective where

$$|Q(j\omega)| \approx 1. \tag{7}$$

In general, the Q-filter is designed as a low-pass filter, which has the dc gain of one, such that the closed-loop system has a good disturbance rejection performance at low frequencies. In this application, we want to have a good control performance up to 8 Hz, which is the frequency bandwidth of a human motion [12]. However, another constraint is imposed on the design of the Q-filter so that the DOB loop is robustly stable. The robust stability condition is

$$|Q(j\omega)| < \frac{1}{|W(j\omega)\Delta(j\omega)|}, \qquad \text{for all } \omega \in R. \tag{8}$$

Therefore, the magnitude and the bandwidth of the Q-filter are dependent on the uncertainties. Since $|\Delta(j\omega)|$ is bounded to one, (8) is satisfied if

$$|Q(j\omega)| < \frac{1}{|W(j\omega)|}, \qquad \text{for all } \omega \in R \tag{9}$$

where $W(j\omega)$ is the uncertainty boundary function designed as in Fig. 6(b). Therefore, the Q-filter is designed such that the magnitude of the Q-filter is smaller than that of the inverse of the uncertainty boundary function for all frequencies ω.

In this application, the magnitude of $W(s)$ is large at low frequencies, which constrains the magnitude of the Q-filter to be less than (9). The dotted line in Fig. 10 shows the magnitude of the inverse of uncertainty boundary function, i.e., $\left|W^{-1}(j\omega)\right|$. Note that $\left|W^{-1}(j\omega)\right|$ is less than one at low frequencies. Since the magnitude of the Q-filter should be one for a good performance, the DOB may not be directly applicable to the control of the flexible transmission system.

To bypass this problem, a proportional–derivative (PD) controller (see C in Fig. 9) is applied to the open-loop system first. The DOB is applied to the closed-loop system that includes the

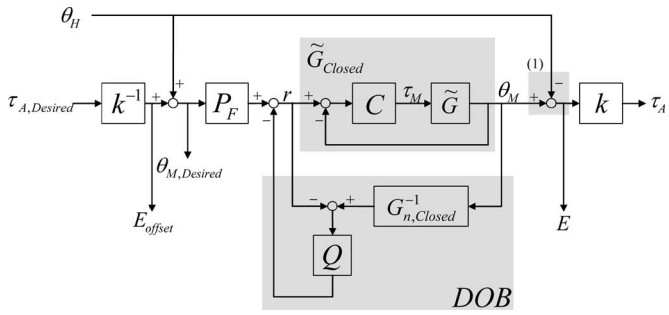

Fig. 9. Block diagram of the overall joint control system [11]. Overall control method is to compensate for impedance in the actuation system in SUBAR. k, C, P_F, and Q represent the spring constant of the flexible transmission, the PD controller, the feedforward filter, and the Q-filter of DOB, respectively.

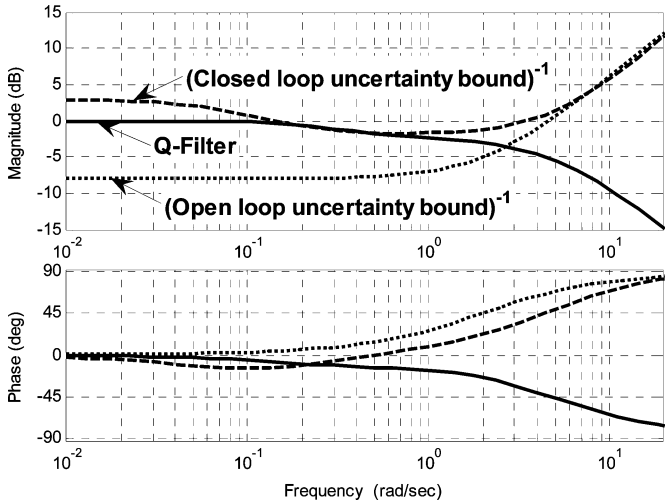

Fig. 10. Bode plot of the Q-filter designed for the flexible transmission.

PD controller, as shown in Fig. 9. In this case, the DOB shapes the reference trajectory (r in the figure) to reject the disturbances imposed on the system. The dashed line in Fig. 10 shows the magnitude of the inverse of uncertainty boundary function of the PD-controlled system. The uncertainty boundary function was obtained by the same method as in Fig. 6. Since the model variation is attenuated by the PD controller (i.e., the magnitude of the inverse of uncertainty boundary function is greater than one at low frequencies), the Q-filter can be designed such that the conditions in (7) and (9) are satisfied, as shown in Fig. 10. Note that the magnitude of the Q-filter is less than that of the inverse of the uncertainty boundary function of the PD-controlled system.

The DOB rejects the model uncertainties by treating them as exogenous disturbances as long as the Q-filter satisfies the conditions in (7) and (8). Since the model variation is significantly reduced by the PD controller and the DOB, a model-based feedforward filter can be employed for better tracking performance. The zero-phase error tracking control (ZPETC) is effective for this purpose. Since the advanced information of human joint angles is not available, the anticasual term in the ZPETC is ignored. For more detailed information on the controller design, see [11].

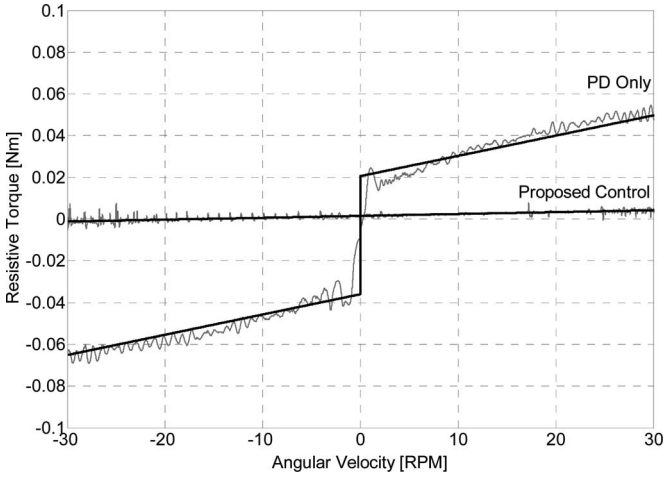

Fig. 11. Controlled resistive torques.

The overall control law is as follows.

1) First, the desired spring deflection (see $E_{\rm offset}$ in Fig. 9) is determined by the main controller that determines the assistive torque. Note that the spring deflection should be determined by considering the gear ratio of (h) and (i) in Fig. 2 (approximately 1:2). The desired position of the motor ($\theta_{M,}$Desired in the figure) is obtained by adding the measured human joint angle (i.e., $\theta_{M,}\text{Desired} = \theta_H + E_{\rm offset}$). Note that if the desired torque is zero, then $\theta_{M,}$Desired is equal to θ_H.
2) Second, the feedforward filter shapes the desired position considering the closed-loop dynamics. In fact, the control performance of the flexible transmission is significantly improved by the feedforward filter.
3) Third, the PD controller is applied to attenuate the large model variation. This enables the Q-filter in the DOB to be designed properly.
4) Finally, the DOB compensates for the remained model variations and rejects other disturbances in the actuation system.

IV. Experimental Verification

A. Model Variation by Human–Robot Interaction

The proposed methods were verified by experiments. By applying the flexible transmission and the associated control algorithm, it is desired to achieve the following performance objectives.

1) The actuation system in SUBAR generates the desired torque precisely.
2) The disturbance such as the friction is rejected such that SUBAR exhibits very low impedance.

To measure how large the generated resistive torque is while the desired torque output is zero, the experimental setup shown in Fig. 4(a) was utilized again. To evaluate the effects of the PD controller and the DOB, experiments were performed without control (i.e., open-loop control), with only the PD controller, and with the proposed controller.

Fig. 11 shows the experimental results of the resistive torque test. Since the resistive torque measured by the open-loop

TABLE II
CALCULATED COEFFICIENTS RELATED TO MECHANICAL IMPEDANCE

	a Bias [Nm]	b Static Friction [Nm]	C Linear Damping [Nm/(rad/s)]
No Control	1.787×10^{-2}	1.214×10^{0}	1.572×10^{-2}
PD Control	-7.725×10^{-3}	2.830×10^{-2}	9.707×10^{-4}
Proposed Control	1.538×10^{-3}	2.237×10^{-5}	8.856×10^{-5}

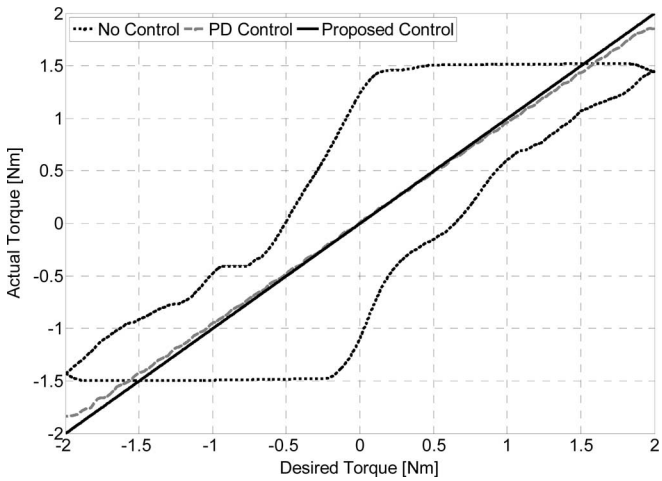

Fig. 12. Controlled relations between desired torque and generated torque.

experiment was too large, the figure compares only the results for the PD control and the proposed control. For the results on the open-loop system, see Fig. 4(b). Note that the proposed control system improves the performance significantly such that the actuation system does not generate large resistive torque, regardless of the magnitude of the angular velocities.

For more quantitative comparison, the data shown in Fig. 9 were analyzed by curve fitting with the following base function:

$$f(v) = a + b\,\mathrm{sgn}(v) + cv \tag{10}$$

where v, a, b, and c represent the angular velocity of the rotor of the flexible transmission, the bias, the friction, and the linear damping, respectively.

Table II shows the coefficients obtained by experiments. The coefficients are obtained by curve fitting based on (10). Fig. 11 shows the fitted curves with thick continuous lines. As expected, the bias, the friction, and the linear damping are significantly decreased by applying the proposed method.

To check if the actuation system generates the desired torque precisely, the experimental setup shown in Fig. 5(a) was utilized. Similarly, the rotor of the RSEA (i.e., the load side of the spring) was locked to observe the relation between the desired torque and the generated torque, while the angular velocity is zero.

Fig. 12 shows the experimental results on the input–output relations. As expected, the proposed control system showed good linearity (see the thick continuous line in the figure). Even though the PD controller compensates for the nonlinearity significantly, it should be noted that the improved precision by the proposed controller is significant in the applications of human–robot interaction for better comfort and safety. The dedicated experiments in Figs. 11 and 12 verify that SUBAR can precisely generate the desired torque by applying the control algorithm discussed in this paper.

TABLE III
CALCULATED RMS ERROR FOR INPUT–OUTPUT LINEARITY TEST

	e_{RMS} [Nm]
No Control	6.734×10^{-1}
PD Control	5.430×10^{-2}
Proposed Control	6.257×10^{-4}

For quantitative evaluation, the amount of nonlinearities was compared by the rms values of errors, i.e.,

$$e_{\mathrm{rms}} = \sqrt{\frac{1}{N}\sum_{i=1}^{N}\left(\tau_{d,i} - \tau_{a,i}\right)^2} \tag{11}$$

where N is the number of samples. $\tau_{d,i}$ and $\tau_{a,i}$ represent the desired and measured torques at the ith sample, respectively.

Table III shows the rms values obtained. Note that the flexible transmission controlled by the proposed method showed the lowest rms value. This implies that the desired torque is precisely generated by applying the proposed methods.

B. Walking Experiment

Dynamic characteristics of the actuation system in SUBAR can be changed by the interaction with a human, as well as the internal model variations discussed in this paper. For example, if a human leg is swinging, it may be regarded as a multiDOF pendulum system. However, if it is touching the ground (e.g., stance phase in a gait), the inertia imposed on the load side of the flexible transmission is increased significantly due to the ground reaction forces.

Since the dynamics of a human body is too complicated to be modeled, the proposed controller for the flexible transmission was designed by treating the unmodeled dynamics as an external disturbance in this paper. However, the dynamics of the human body may be able to introduce instability to the actuation system. If a human is severely impaired so that he/she cannot generate a lot of muscular power, then the system may be stable by the passivity theory [16]. In actual cases, however, nothing can be assumed or guaranteed.

Therefore, it is important to ensure the stability and the performance of human-centered robots by experiments. In the case of SUBAR, the model variation caused by the dynamics of the human body is to be compensated by robustness of the DOB. To verify performance of the proposed method in actual cases, a healthy young subject wearing SUBAR walked at a normal speed, as shown in Fig. 13. Fig. 14 shows the experimental results on a hip joint during walking. The desired torque was set to zero (i.e., the desired deflection of the flexible transmission was zero) to check how large resistive torque is generated during the human motions. In an ideal case, it is expected that no resistive

Fig. 13. Walking experiment by a human subject.

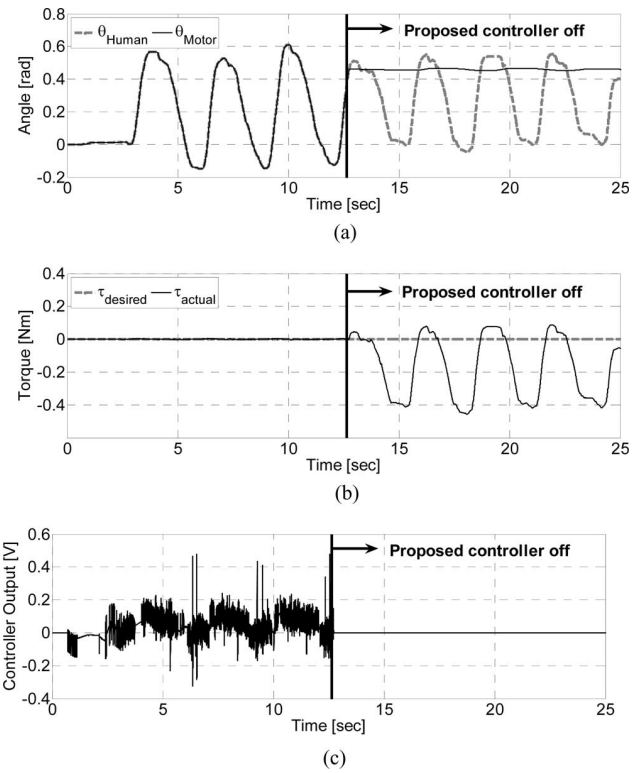

Fig. 14. Experimental results: Desired torque was set to zero. (a) Human joint motion and motor position. (b) Resistive torque generated during motion. (c) Controller output.

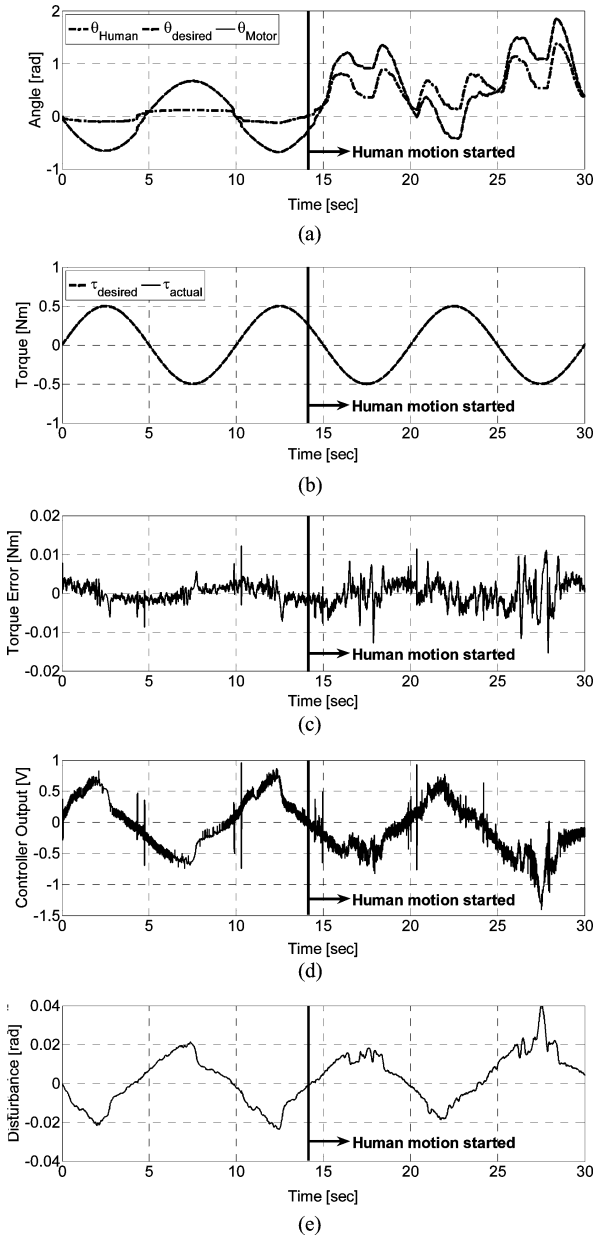

Fig. 15. Experimental results: Smoothened step functions were applied as the desired torque. (a) Motor angle and human joint angle. (b) Desired and actual torques. (c) Error between desired and actual torques. (d) Controller output. (e) Observed disturbance by DOB.

torque is generated, regardless of human motion. Fig. 14(a) shows the hip joint motion during walking and the motor position controlled by the proposed method. Since the desired deflection was zero, the motor followed the human joint motion without offset. Fig. 14(b) shows the generated resistive torque, which is calculated by multiplying a spring constant to the deflection of the flexible transmission [i.e., $k(\theta_{\mathrm{Motor}} - \theta_{\mathrm{Human}})$]. Fig. 14 compares the performance with and without the proposed controller. Note that the resistive torque, which was observed when the control algorithm was suppressed [see after 12.5 s in Fig. 14(b)], was successfully compensated by the control algorithm (see before 12.5 s in the figure). Even though small resistive torque was still observed even with the proposed method, the magnitude of resistive torque was significantly decreased by applying the proposed method. The residual resistive torque might occur because of 1) ignorance of the anticausal term in the feedforward filter and 2) the limitation of the bandwidth of the Q-filter in DOB. It should be noted that the controller robustly controlled the flexible transmission, even when environment interacted with a human. Note that the output of the proposed controller was chattering, as shown in Fig. 14(c). This might have been caused by quantization error of the encoders, which is amplified by the feedforward filter (see P_F in Fig. 9). It is possible to reduce the chattering effect by decreasing the bandwidth of the feedforward filter. However, the limited bandwidth decreases the control performance so that the resistive torque is not effectively eliminated. In the experiment in this paper, the bandwidth of the feedforward filter was selected such that the actuator does not generate any noise, while the resistive torque is effectively eliminated.

In Figs. 14 and 15, the stimulus includes the human-side motion as well as the desired assistive torque. Note that actuators should respond to both human motion and desired torque for improved comfort and safety. In Fig. 15, to compare the performance with respect to the human motion and the desired torque, the desired torque was set to a sinusoidal wave with a low frequency, where the human motion had the frequency component of 0.5 Hz, which is the normal natural frequency of patients' walking motion. In Fig. 15(a), note that the motor was controlled to have the offset, which is proportional to the desired torque. It should be also noted that the proposed method generated the desired torque precisely under the environment interacting with a human. Fig. 15(c) shows an error between the desired and the generated torques. The magnitude of error was 0.00282 Nm in rms and 0.56% of the desired torque level. Note that the magnitude of error was slightly increased after the human motion started. This might be because of the variations of effective inertia of the human body. Also note that the disturbance measured by the DOB was slightly different after the human motion started. Since the DOB was applied to a PD closed-loop system, the unit is in radians, as shown in the figure. Therefore, the DOB is to modify the desired spring deflection for appropriate compensation of the friction and the inertia of actuators.

V. Conclusion and Future Works

In order to reduce the mechanical impedance of SUBAR, a flexible transmission and its associated controller were designed. For precise generation of the assistive torque, the deflection of the flexible transmission was controlled to have the desired offset by a robust servo controller. By the flexible transmission and associated control algorithms discussed in this paper, SUBAR exhibited very low impedance, while the desired torque was generated precisely. The performance of the proposed method was verified by experiments in this paper.

The controller proposed in [11] has been shown to work well in the SUBAR system. It enables an ideal force-mode actuation for improved human–robot interaction, which is required for assisting patients. The higher level algorithms that determine the assistive torques are under development and will be clinically verified on patients in our future work.

References

[1] K. Kong and D. Jeon, "Design and control of an exoskeleton for the elderly and patients," *IEEE/ASME Trans. Mechatron.*, vol. 11, no. 4, pp. 428–432, Aug. 2006.

[2] K. Kong and D. Jeon, "Fuzzy control of a new tendon-driven exoskeletal power assitive device," in *Proc. IEEE/ASME Int. Conf. Adv. Intell. Mechatron.,* 2005, pp. 146–151.

[3] M. Zinn, O. Khatib, and B. Roth, "A new actuation approach for human friendly robot design," in *Proc. IEEE Int. Conf. Robot. Autom.*, 2004, pp. 249–254.

[4] M. Zinn, O. Khatib, B. Roth, and J. K. Salisbury, "Actuation methods for human-centered robotics and associated control challenges," *Control Problems Robot.*, vol. 4, pp. 105–119, 2003.

[5] R. Riener, L. Lunenburger, S. Jezemik, M. Anderschitz, G. Colombo, and V. Dietz, "Patient-cooperative strategies for robot-aided treadmill training: First experimental results," *IEEE Trans. Neural Syst. Rehabil. Eng.*, vol. 13, no. 3, pp. 380–394, Sep. 2005.

[6] N. Hogan, "Stable execution of contact tasks using impedance control," in *Proc. IEEE Int. Conf. Robot. Autom.*, 1987, pp. 1047–1054.

[7] S. P. Buerger and N. Hogan, "Complementary stability and loop shaping for improved human–robot interaction," *IEEE Trans. Robot. Autom.*, vol. 23, no. 2, pp. 232–244, Apr. 2007.

[8] J. Blaya and H. Herr, "Adaptive control of a variable-impedance ankle–foot orthosis to assist drop-foot gait," *IEEE Trans. Rehabil. Eng.*, vol. 12, no. 1, pp. 24–31, Mar. 2004.

[9] K. Kong and M. Tomizuka, "Flexible joint actuator for patient's rehabilitation device," in *Proc. IEEE Int. Conf. Robot Human Interactive Commun.*, 2007, pp. 1179–1184.

[10] K. Kong, J. Bae, and M. Tomizuka, "Impedance compensation of flexible joint actuator for ideal force mode control," in *Proc. 17th Int. Fed. Autom. Control World Congr.*, 2008, pp. 2442–2447.

[11] K. Kong, J. Bae, and M. Tomizuka, "Control of rotary series elastic actuator for ideal force mode actuation in human-robot interaction applications," *IEEE/ASME Trans. Mechatron.*, vol. 14, no. 1, pp. 105–118, Feb. 2009.

[12] D. Winter, *Biomechanics and Motor Control of Human Movement*. New York: Wiley-Interscience, 1990.

[13] K. Kong and M. Tomizuka, "Smooth and continuous human gait phase detection based on foot pressure patterns," in *Proc. IEEE Int. Conf. Robot. Autom.*, 2008, pp. 3678–3683.

[14] J. Pratt, B. Krupp, and C. Morse, "Series elastic actuators for high fidelity force control," *Int. J. Ind. Robot*, vol. 29, no. 3, pp. 234–241, 2002.

[15] G. A. Pratt and M. W. Williamson, "Series elastic actuators," in *Proc. IEEE/RSJ Int. Conf. Intell. Robot. Syst.*, 1995, vol. 1, pp. 399–406.

[16] J. Ryu, D. Kwon, and B. Hannaford, "Stability guaranteed control: Time domain passivity approach," *IEEE Trans. Control Syst. Technol.*, vol. 12, no. 6, pp. 860–868, Nov. 2004.

Kyoungchul Kong (S'04) received the B.Eng. degree (*summa cum laude*) in mechanical engineering and the B.S. degree in physics, both in 2004, and the M.S. degree in mechanical engineering in 2006 from Sogang University, Seoul, Korea. He is currently working toward the Ph.D. degree in mechanical engineering, University of California, Berkeley.

He has authored or coauthored about 40 technical articles published in journals and conference proceedings. His current research interests include the design, modeling, and control of mechatronic systems with emphasis on the betterment of the quality of human life.

Hyosang Moon (S'08) received the B.Eng. degree in mechanical engineering in 2007 from Sogang University, Seoul, Korea, where he is currently working toward the M.S. degree.

His current research interests include the design and control of human-interactive robotics such as rehabilitation robots and exoskeleton systems.

Beomsoo Hwang (S'07) received the B.Eng. degree in mechanical engineering in 2007 from Sogang University, Seoul, Korea, where he is currently working toward the M.S. degree.

His current research interests include sensors for biomechatronics systems, and the design and control of human-interactive robotics such as rehabilitation robots and exoskeleton systems.

Doyoung Jeon (S'86–M'92) received the B.S. degree from Seoul National University, Seoul, Korea, in 1984 and the M.S. and Ph.D. degrees from the University of California, Berkeley, in 1986 and 1991, respectively, all in mechanical engineering.

In 1994, he joined the Department of Mechanical Engineering, Sogang University, Seoul, where he was the Dean of Research from 2004 to 2005. His current research interests include the general areas of control systems, such as exoskeletal robots, rehabilitation robots, capsule endoscopes, and servo control of advanced manufacturing machines.

Prof. Jeon was a committee member of the Korean Presidential Advisory Council on Science and Technology from 2005 to 2006 and the Korean Presidential Commission on Policy Planning from 2002 to 2008.

Masayoshi Tomizuka (M'86–SM'95–F'97) received the B.S. and M.S. degrees from Keio University, Tokyo, Japan, in 1968 and 1970, respectively, and the Ph.D. degree from the Massachusetts Institute of Technology, Cambridge, all in mechanical engineering.

In 1974, he joined the Department of Mechanical Engineering, University of California, Berkeley, where he is currently the Cheryl and John Neerhout, Jr., Distinguished Professor Chair. His current research interests include optimal and adaptive control, digital control, signal processing, motion control, and control problems related to robotics, machining, manufacturing, and information-storage devices and vehicles.

Prof. Tomizuka was the Editor-in-Chief of the IEEE/AMERICAN SOCIETY OF MECHANICAL ENGINEERS (ASME) TRANSACTIONS ON MECHATRONICS from 1997 to 1999. He is a Fellow of the ASME and the Society of Manufacturing Engineers. He was the recipient of the Charles Russ Richards Memorial Award from ASME in 1997, the Rufus Oldenburger Medal from ASME in 2002, and the John R. Ragazzini Award in 2006.